Non-dimensionalized distances and limits for transition of deflagration to detonation

Vincent Rodriguez, Vianney Monnier, Pierre Vidal, Ratiba Zitoun

Noname manuscript No.
(will be inserted by the editor)

Towards non-dimensionalized distances and limits for transition of deflagration to detonation

V. Rodriguez · V. Monnier · P. Vidal · R. Zitoun

Received: date / Accepted: date

Abstract This experimental work investigates the possibility to non-dimensionalize the limits and the distances of the Deflagration-to-Detonation-Transition process (DDT). The deflagration was ignited using jets of hot gases generated by the impact of a Chapman-Jouguet detonation on a multi-perforated plate. Small holes were uniformly distributed on the plate, over the whole tube section. The tube was 1-m long with square cross-section 40×40 mm^2. The reactive mixtures were the stoichiometric compositions of hydrogen, methane and oxygen $(1\text{-}x)\mathrm{H_2} + x\,\mathrm{CH_4} + \frac{1}{2}\,(1+3\,x)\mathrm{O_2}$ with the composition parameter x ranging from 0 to 1. The initial pressure p_0 was varied from 12 to 35 kPa, and the initial temperature was 294 K. The re-ignition conditions and distances were obtained as functions of x, p_0 and the plate properties. The mean widths of the detonation cells measured at the wall were used to non-dimensionalize the DDT distances, the surface of the perforations and the surface of the walls of the plate holes. This non-dimensional DDT distance thus appears to be a concave increasing function of the non-dimensional perforated surface independent of the regularity of the cellular structure. DDT processes are very dependent on the system configuration and the ignition conditions but our analysis suggests that the proper selection of non-dimensional numbers built from the system characteristics can help in anticipating the corresponding DDT limits and distances to a reasonable approximation.

E-mail: vincent.rodriguez@ensma.fr
V. Rodriguez · V. Monnier · P. Vidal · R. Zitoun
Institut Pprime, UPR 3346 CNRS, ENSMA, BP 40109, 86961 Futuroscope-Chasseneuil, France

Keywords deflagration · detonation · cellular structure · non-dimensionalization · hot-gas jets

1 Introduction

Understanding the onset of fast flame and deflagration, and their transition to detonation in tubes, is one of the oldest motivations for studying quasi-sonic and supersonic combustion waves. The main phenomena that participate in the deflagration and detonation processes, and the transitions from the former to the latter, are well understood qualitatively today. However, each remains a numerical challenge and predicting how they combine in complex reactive flows is currently out of reach. The prevailing approach today is to address and model the DDT processes jointly with simplified macroscopic analyses to bring out salient relevant parameters.

Ciccarelli and Dorofeev [5] presented a review of DDT processes that includes the pioneering works by Shchelkin. The DDT phenomenological stages are now agreed to depend on the roughness of the tube walls and the transverse dimension of the tube relative to some reference reaction thickness. Most laboratory DDT processes are triggered using low-energy ignition techniques, such as an automotive spark plug. In smooth tubes, for large enough transverse dimensions, the dynamics of the initial flame is then subjected to strong effects of curvature and acceleration, a shock forms ahead of the flame front, an overdriven detonation suddenly forms between the flame and the shock, propagates in the transverse and backward direction with respect to the frontward-propagating leading shock, and this complex eventually relaxes to the CJ detonation regime [11,12]. The overdriven detonation usually forms at the tube

wall, and preferentially at the inner edges of square or rectangular tubes. This indicates that the dissipation effects in boundary layers have also a strong influence on the flame acceleration. Obviously enough, such effects are more effective at wall intersects than at surfaces. For narrow enough tubes and low enough energy of ignition, the transition process can include a quasi-steady, slowly-accelerating, quasi-planar combustion wave with velocity about one-half that of the CJ detonation – the so-called "strange wave" – before sudden one-dimensional transition to the CJ detonation regime, without precursor shock [13,14,15].

The DDT phenomenon is thus a set of individually complex processes, and the objective of our work is to conduct and analyze experiments to determine whether a proper choice of dimensionless parameters could represent the transition limits and lengths. Our investigation is restricted to the DDT process generated by jets of hot gases uniformly distributed over most of the cross section of a smooth-wall square tube. These hot jets were obtained from the impact of a CJ detonation on a perforated plate. This choice of surface ignition of the initial subsonic flame front ensures a simpler hydrodynamic field ahead of the front and, therefore, a better reproducibility of the transition limits and lengths. In these conditions, our aim is to obtain macroscopic information on the transition limits and lengths rather than the detailed dynamics of the re-ignition processes.

For similar conditions, the literature review brings out that the main control parameters are the number of holes in the plate, the width λ_{CJ} of the detonation cell, as compared to both the transverse dimension of the tube and the diameter of the holes, and the regularity $\Delta\lambda_{CJ}/\lambda_{CJ}$ of the detonation cells (the standard deviation of their mean width). A regularity criterion is defined from the ZND model of the planar detonation reaction zone by the ratio χ of the reaction thickness to that of the induction [21,22], and this regularity increases with decreasing χ. For example, $\chi = 350$ for the irregular $CH_4 + 2\,O_2$ mixture and $\chi = 7$ for the regular $2\,H_2 + O_2$ mixture at the initial pressure 20 kPa. Overall, the re-ignition distance R then seems to decrease with decreasing λ_{CJ} and regularity, that is, re-ignition seems easier with more irregular mixtures [3,19,10,16]. The two main re-ignition mechanisms after the incident detonation has quenched through the plate are the interactions of the diffracted shocks with themselves and the walls of the tube [1,2,4]. In particular, Medvedev et al. [17] identified (i) a direct detonation initiation in the zone of turbulent mixing between the jets of the combustion products and the fresh mixture and (ii) a detonation initiation from localized explosions resulting from the interaction between the jets and the shock waves reflected at the bounding walls.

Kuznetsov et al. [12] observed that R decreases with decreasing λ_{CJ} for the stoichiometric H_2–O_2 mixture, and they noted the prominent effect of a turbulent boundary layer before re-ignition. Chao et al. [3] observed that R is shorter with irregular mixtures – H_2/Air – than with regular mixtures – H_2/ O_2. Sentanuhady et al. [23] used plates with thickness 5 mm and diameters d ranging from 1 mm to 5 mm. They found that R is shorter with multiple-perforated plates than with single-hole plates, but they did not detail the effects of the plate thickness and the hole diameter. It should be noted that their plates had hole diameters larger than the cell widths. Grondin and Lee [6] proposed two onset mechanisms based on schlieren visualizations. For regular cells, the reaction-zone regenerates within a thin planar layer normal to the main propagation direction without precursor shock. For irregular cells, the regeneration is three-dimensional with distributed burnt and unburnt pockets that coalesce to achieve the CJ detonation regime. Their experimental conditions were such that re-ignition was very close to the plate – about two to three λ_{CJ} –, so their results are more representative of the last stage of the DDT process.

The open area ratio (OAR, ratio of the total area of holes to the cross-section area) is often considered for characterizing DDT. However, detonation has been often observed to quench inside the perforated plates if the cell width λ_{CJ} is bigger or equal to the diameter d of the holes [7,8,9]. Therefore, the same OAR may result or not in detonation quenching, so the OAR cannot be the only parameter for characterizing DDT ignition.

We thus determined the transition distances R and limits behind a multi-perforated plate using stoichiometric compositions of hydrogen, methane and oxygen $(1\text{-}x)H_2 + x\,CH_4 + \frac{1}{2}\,(1+3\,x)O_2$. We varied the composition parameter x from 0 to 1 to generate detonation cells ranging from regular ($x = 0$, $H_2 + \frac{1}{2}\,O_2$) to irregular ($x = 1$, $CH_4 + 2\,O_2$), according the usual characterization. We varied the initial pressure p_0 from 12 to 35 kPa, and the initial temperature was ~ 294 K. We choose perforated plates with hole diameters d smaller than the cell widths λ_{CJ}, so the detonation quenched through the plate. Therefore, the possible re-ignition behind our plates result from jets of burnt gases. In a first series of experiments, we kept constant the properties of the perforated plates, namely their thickness e, and the hole number N and diameter and d, and we studied the effects of varying p_0 and the composition parameter x. In a second series of experiments, we selected the more regular mixture, that is, $x = 0$ ($H_2 + \frac{1}{2}\,O_2$), and we studied the effects of varying the proper-

ties of the perforated plate e, N and d. For both of the series, we kept constant the open area ratio (OAR).

Section 2 describes the experimental set-up, section 3 is the analysis of the results that brings out a non-dimensional representation of the DDT limits and distances based on the properties of the cellular structure and the perforated plate, and section 4 discusses and concludes this work.

2 Experimental methodology

The experimental set-up is a detonation tube that consists of two main elements, namely the driver section and the re-ignition section separated by the perforated plate (Fig.2). The methodology is to generate detonation at one end of the driver section, to quench it through the plate, and to study the conditions for re-ignition depending on the properties of the plate, the composition of the mixture and the initial pressure p_0. The driver and re-ignition sections are 2.25 and 1-m long, respectively, with square cross-section 40×40 mm^2. Figure 1 shows a schematic of the experimental set-up, and table 1 gives the properties of the perforated plates. The detonation in the driver section resulted from the deflagration generated by the spark of an automotive plug, and transition to detonation was then obtained by a 1-m long Shchelkin spiral positioned immediately ahead of the plug. The set-up was vacuumed before injecting the premixed composition prepared in a separate tank using the partial-pressure method. Three Kistler 603B pressure transducer (1 μs response time, 300 kHz natural frequency, each coupled with a Kistler 5018 A electrostatic charge amplifier with 200 kHz band width) were used to check that the CJ detonation regime was achieved before the plate. The transducer P3 is located 125 mm before the plate, and the distance between each transducer (P1, P2 and P3) is 250 mm.
The reactive gases were the stoichiometric mixtures of hydrogen-methane-oxygen initially at T_0 ∼294 K:

$$(1\text{-}x)\mathrm{H_2} + x\,\mathrm{CH_4} + \frac{1+3\,x}{2}\mathrm{O_2} \longrightarrow x\,\mathrm{CO_2} + (1+x)\mathrm{H_2O} \tag{1}$$

Five compositions were studied, namely $x = 0$, 0.25, 0.5, 0.75 and 1 (Table 2). Soot-covered foils positioned on the bottom faces of the driver and the re-ignition sections were used to record the structure of the detonation cells upstream and downstream the plate, and to obtain the cell widths.

Figure 3 shows soot-foil recordings upstream the plate, at initial pressure $p_0 = 25$ kPa. Depending on the mixture, that is, on the value of the composition parameter x, the wall recordings show how the cell width and irregularity increase with increasing x, that with decreasing amount of H_2 and increasing amount of CH_4.

Figure 4 shows a typical soot recording at the position of the final stage of the DDT. Here, the detonation re-ignition occurs at the bottom wall. The cells are first very small, which indicates that this initial detonation is overdriven. They eventually become parallel to the tube axis, with larger and essentially constant width, which indicates that the detonation attains the self-sustained regime.

3 Results

The premise of the analysis below is that the re-ignition process results essentially of the interplay of two competing phenomena, namely nonadiabatic surface dissipation versus hot spots and chemical heat release, that is, dissipation effects at the tube walls and inner edges versus chemically-enhanced shock amplification. They are described by means of a dimensional analysis that involves chemical and geometrical lengths, namely the cell mean width λ_{CJ}, and the thickness e and the diameter d of the holes in the plate. The number of holes N is also an important parameter. Table 1 shows the values of e, d, and N. Surface dissipation take place at the walls of the holes in the plate and at those of the re-ignition section of the tube, between the plate and the position of re-ignition. The total exchange surface in the plates is $N\pi\,d\,e$, and the product $N\,d\,e$ is a measure of these nonadiabatic exchanges. This dimensionless analysis includes only the contribution of the exchange surface of the holes because it is much larger than that of the tube, per unit length. Further, all experiments were carried out in the same tube, so the results cannot be used to anticipate the re-ignition distances in a tube with a different cross-section or that would be made up of another material, or with rough walls. Hot-gas jets form when the flow exits the holes, and they interact at a distance that depends on the mixture composition and the initial pressure and temperature. The initial total surface of the jets is $N\pi\,d^2/4$, and the product Nd^2 is a measure of the surface formed by the interaction of the jets. The analysis considers dimensionless ratios that use the cell mean width λ_{CJ} as the reference length for representing the effect of heat production by evolution of chemical composition. These ratios are (i) Nd^2/λ_{CJ}^2 for the relative effects of surface re-ignition resulting from the interaction of the jets coming out of the holes, and (ii) $Ne\,d/\lambda_{CJ}^2$ for the relative effects of the surface-dissipation phenomenon.

Figure 5 shows the domains of re-ignition and non-re-ignition in the λ_{CJ}-x plane. The data were obtained by varying the initial pressure p_0 at constant composition x, so the figure also indicates the dependence of λ_{CJ} on the composition parameter x and the initial pressure p_0. The cell width λ_{CJ} thus appears to be a linear increasing function of x at fixed p_0, and to increase with decreasing p_0 at fixed x. The values of λ_{CJ} that separate the re-ignition and non-re-ignition domains form a convex increasing function of x. The limiting pressures at its intersects with the constant-p_0 lines decrease with increasing x, that is, with increasing λ_{CJ}. Therefore, the less regular the cells (the larger x), the smaller the limiting pressure. Figure 6 shows the domains of re-ignition and non-re-ignition in the plane Nd^2/λ_{CJ}^2-Ned/λ_{CJ}^2. The data were obtained with the same composition $x = 0$ by varying the parameters N, d, e, and p_0. Each point in the graph corresponds to the change of one parameter only (Table 1). The results suggest that the value of Nd^2/λ_{CJ}^2 that separates re-ignition and non-re-ignition is independent of the dimensionless number Ned/λ_{CJ}^2. Therefore, to within a reasonable accuracy, the limiting dimensionless number (full line) for the surface re-ignition effects appears to be independent of the dimensionless number for the surface-dissipation effects in the plate. However, as discussed next, the re-ignition distance depends on both effects of the surface dissipation and the surface re-ignition.

For a given composition of the mixture, the properties of the plate, precisely its nonadiabatic inner processes and the interaction effects at its exit, strongly influence the mechanisms of combustion re-ignition (hot-gas jets, flame structure and development) and, therefore, the transition distance to detonation. In contrast, the variations of the mixture composition, for the same plate, result in a limited dispersion of the DDT limits and length.

Figure 7 shows the re-ignition distance R as a function of the mean width of the detonation cell λ_{CJ}, with the composition parameter x varying from 0 to 1 (the tube length L was the same in all experiments, hence its more convenient representation by the ratio R/L). The slopes of the approximation curves through the points associated to a same value of x increase with decreasing x, that is, the transition distance is all the more sensitive to the cell width as the mixture is more regular. Figure 9 also illustrates this trend as the re-ignition distance R non-dimensionalized by λ_{CJ} and plotted as a function of λ_{CJ}.

Figure 8 shows the non-dimensionalized re-ignition distance R/λ_{CJ} as a function of the non-dimensionalized ratio d^2/λ_{CJ}^2 representing the relative effects of surface re-ignition, for plate (A). A good alignment is observed regardless the value of x from 0 to 1. Fig.10 shows this interesting property extends to all the plates considered in this study.

In our conditions, the thickness of the perforated plate does not appear to significantly influence the re-ignition distance R. Medvedev et al. [17] suggested that this occurs for plate thicknesses e ranging in e/d=2 - 8 (d is the diameter of a hole), and indeed e/d=2.33 - 7 in our experiments.

4 Discussion and conclusions

This work reports on experiments on the deflagration-to-detonation transition in a square cross-section channel. Our goal was to investigate the possibility of non-dimensionalizing the DDT limits and distances using simple observable characteristics parameters. Ignition was achieved using jets of hot gases generated by quenching CJ detonation through a perforated plate. Thus, the parameters involved in our analysis are the CJ cell width, the thickness of the plates, the number and diameter of the holes in the plates, and the composition parameter. In our conditions, analysis evidences that the non-dimensional DDT limits, that is, the re-ignition and non-re-ignition, are independent of the relative effects of the surface dissipation phenomena in the holes, and that the non-dimensional DDT distances well correlate with the non-dimensional number Nd^2/λ_{CJ}^2 representing the relative effects of surface re-ignition resulting from the interaction of the jets coming out of the holes. Additionally, this non-dimensionalization appears to be independent of the regularity of the detonation cell, as defined by soot recordings at walls. This indicates that this regularity criterion may not always be relevant for interpreting dynamical behaviours of deflagration and detonation [28].

In general, DDT dynamics depends on the ignition mode, the set-up geometry and dimensions, and the mixture composition, so only high-resolution numerical simulations based on Navier-Stokes reactive equations will be capable of predicting this complex phenomenon when the necessary computations capacities are available. To date, given an industrial system, the DDT risk must be assessed with large-scale model experiments. In this respect, our analysis suggests that the proper selection of non-dimensional numbers built from the system characteristics can help in anticipating the corresponding DDT limits and distances.

Acknowledgements Part of this work was supported by a CPER-FEDER Project of Région Nouvelle Aquitaine.

References

1. T. Obara, J. Sentanuhady, Y. Tsukada, S. Ohyagi, re-ignition process of detonation wave behind a slit-plate, Shock Waves, 18, 63-83 (1982)
2. R.R. Bhattacharjee, S.S.M. Lau-Chapdelaine, G. Maines, L. Maley, M.I. Radulescu, Detonation re-initiation mechanism following the Mach reflection of a quenched detonation, Proceedings of the Combustion Institute, 34, 1893-1901 (2013)
3. J. Chao, Critical deflagration waves that lead to the onset of detonation, PhD thesis, McGill University, Montreal, DC, Canada (2006)
4. G. Ciccarelli, J.L. Boccio, Detonation wave propagation through a single orifice plate ina circular tube, Twenty-Seventh Symposium (International) on Combustion, The Combustion Institute, 2233-2239 (1998)
5. G. Ciccarelli, S. Dorofeev, Flame acceleration and transition to detonation in ducts, Progress in Energy and Combustion Science, 34, 499-550 (2008)
6. J.S. Grondin, J.H.S. Lee, Experimental observation of the onset of detonation downstream of a perforated plate, Shock Waves, 20, 381-386 (2010)
7. S.V. Khomik, B. Veyssiere, S.P. Medvedev, V. Montassier, H. Olivier, Limits and mechanism of detonation re-initiation behind a multi-orifice plate, Shock Waves, 22, 199-205 (2012)
8. S.V. Khomik, B. Veyssiere, S.P. Medvedev, V. Montassier, G.L. Agafonov, M.V. Silnikov, On some conditions for detonation initiation downstream of a perforated plate, Shock Waves, 23, 207-211 (2013)
9. S.V. Khomik, S.P. Medvedev, B. Veyssiere, H. Olivier, O.G. Maksimova, M.V. Silkikov, Initiation and suppression of explosive processes in hydrogen-containing mixtures by means of permeable barriers, Russian Chemical Bulletin, International Edition, 63, 1666-1676 (2014)
10. M.S. Kuznetsov, V.I. Alekseev, S.B. Dorofeev, Comparison of critical conditions for DDT in regular and irregular cellular detonation systems, Shock Waves, 10, 217-223 (2000)
11. M.S. Kuznetsov, I. Matsukov, V.I. Alekseev, W. Breitung, S. Dorofeev. Effect of boundary layer on flame acceleration and DDT. In: CDROM. Proceedings of 20th international colloquium on the dynamics of explosions and reactive systems (ICDERS), Montreal (2005).
12. M.S. Kuznetsov, V.I. Alekseev, I. Matsukov, DDT in a smooth tube filled with a hydrogen-oxygen mixture, Shock Waves, 14, 205-215 (2005)
13. J. Yanez, M.S. Kuznetsov, Experimental study and theoretical analysis of a 'strange wave', Combustion and Flame, 167, 494-496 (2016)
14. H. W. Ssu, M. H. Wu, Fomation and characterisation of composite reaction-shock clusters in narrow channels, Proceedings of the Combustion Institute, 38, 3473-3480 (2021)
15. Y. Ballossier, F. Virot, J. Melguizo-Gavilanes, Strange wave formation and detonation onset in narrow channels, Journal of Loss Prevention in Process Industries, 72, 104535 (2021)
16. L. Maley, R. Bhattacharjee, S.M. Lau-Chapdelaine, M.I. Radulescu, Influence of hydrodynamic instabilities on the propagation mechanism of fast flames, Proceedings of the Combustion Institute, 35, 2117-2126 (2015)
17. S.P. Medvedev, S.V. Khomik, H. Olivier, A.N. Polenov, A.M. Bartenev, B.E. Gelfand, Hydrogen detonation and fast deflagration triggered by turbulent jet of combustion products, Shock Waves, 14, 193-203 (2005)
18. M.I. Radulescu, J.H Lee, The failure mechanism of gaseous detonation: experiments in porous wall tubes, Combustion and flame, 131, 29-46 (2002)
19. M.I. Radulescu, G.J. Sharpe, J.H.J Lee, C.B. Kiyanda, A.J. Higgins, R.K. Hanson, The ignition mechanism in irregular structure gaseous detonations, Proceedings of the Combustion Institute, 30, 1859-1867 (2005)
20. M.I. Radulescu, B.McN. Maxwell, The mechanism of detonation attenuation by a porous medium and its subsequent re-initiation, J. Fluid Mech., 667, 96-134 (2011)
21. M. Short, G. J. Sharpe, Pulsating instability of detonation with a two-step chain-branching reaction model: theory and numerics, Combustion Theory and Modeling, 7, 401-416 (2013)
22. M.I. Radulescu, G.J. Sharpe, D. Bradley, A universal parameter quantifying hazards, detonability and hot spot formation: the χ number, Proceedings of the Seventh International Seminar on Fire and Explosion Hazards (ISFEH7) (2013)
23. J. Sentanuhady, Y. Tsukada, T. Yoshihashi, T. Obara, S. Ohyagi, Re-initiation of detonation waves behind a perforated plate, Proceedings of the 20^{th} International Colloquium on th Dynamics of Explosion and Reactive Systems (ICDERS), vol. 20, p 1-4 (2005)
24. R.I. Soloukhin, Ignition and detonation processes in the interaction of shock waves with perforated plates, Acta Astronautica, 1, 249-258 (1974)
25. R.A. Strehlow, C.D. Engel, Transverse waves in detonations: II. Structure and spacing in H2-O2, C2H2-O2, C2H4-O2, and CH4-O2 systems, AIAA Journal, 7, 492-496 (1969)
26. L.Q. Wang, H.H. Ma, Z.W. Shen, M.J. Lin, X.J. Li, Experimental study of detonation propagation in a square tube filled with orifice plates, International Journal of Hydrogen Energy, 43, 4645-4656 (2018)
27. L.Q. Wang, H.H. Ma, Z.W. Shen, D.G. Chen, Effect of a single orifice plate on methane-air explosion in a constant volume vessel: position and blockage ratio dependence, International Journal of Hydrogen Energy, 43, 4645-4656 (2018)
28. V. Monnier, V. Rodriguez, P. Vidal, R. Zitoun, Experimental analysis of cellular detonations: regularity and 3D patterns depending on the geometry of the confinement, extended abstract submitted to the 28^{th} International Colloquium on the Dynamics of Explosion and Reactive Systems (ICDERS), Napoli (2022)

Table 1 Properties of the perforated plates used to generate the hot-gas jets.

plates	thickness e (mm)	hole number N	hole diameter d (mm)	OAR
A	7	64	3	28%
B	7	144	2	28%
C	14	64	3	28%
D	21	64	3	28%

Table 2 Composition of the stoichiometric hydrogen-methane-oxygen mixtures $(1\text{-x})H_2 + xCH_4 + \frac{1}{2}(1+3\,x)O_2$.

n°	x	composition for $\Phi = 1$	$\%H_2$	$\%CH_4$	$\%O_2$
1	0	$H_2 + 0.5\,O_2$	0.667	0	0.333
2	0.25	$0.75\,H_2 + 0.25\,CH_4 + 0.875\,O_2$	0.4	0.13	0.47
3	0.5	$0.5\,H_2 + 0.5\,CH_4 + 1.25\,O_2$	0.22	0.22	0.56
4	0.75	$0.25\,H_2 + 0.75\,CH_4 + 1.625\,O_2$	0.095	0.286	0.619
5	1	$CH_4 + 2\,O_2$	0	0.333	0.667

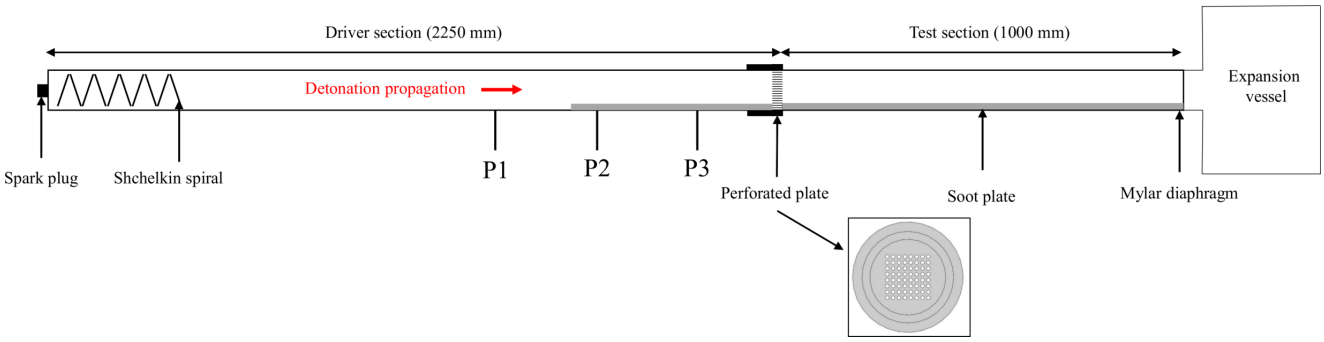

Fig. 1 Schematic of the experimental set-up. Channel cross-section: 40 × 40 mm^2, P1, P2 and P3: pressure gauges.

Fig. 2 Perforated plate (plate B, Table 1).

Fig. 3 Upstream soot-foil recordings showing the detonation cellular structure depending on the composition x of the mixtures $(1\text{-x})H_2 + xCH_4 + \frac{1}{2}(1+3\,x)O_2$ at initial pressure $p_0 = 25$ kPa.

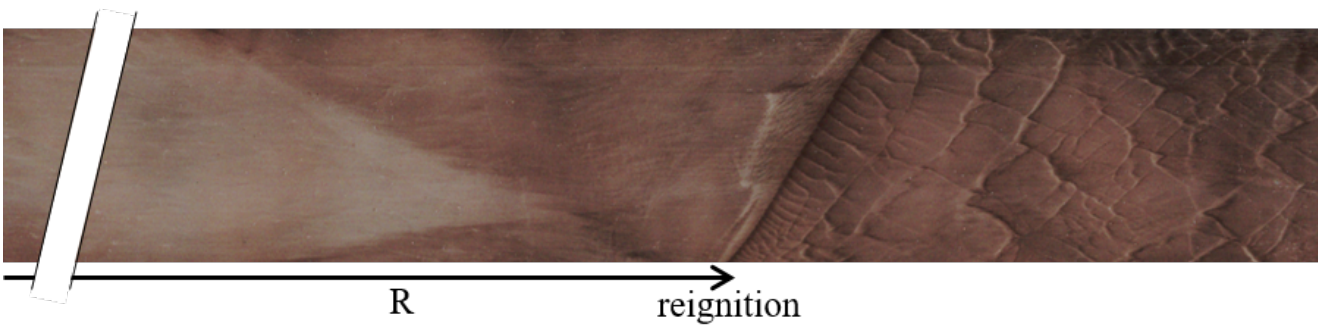

Fig. 4 Downstream soot-foil recording showing detonation re-ignition. $x = 1$ $(CH_4 + 2\,O_2)$ at initial pressure $p_0 = 17.5$ kPa. R is the DDT distance from the perforated plate.

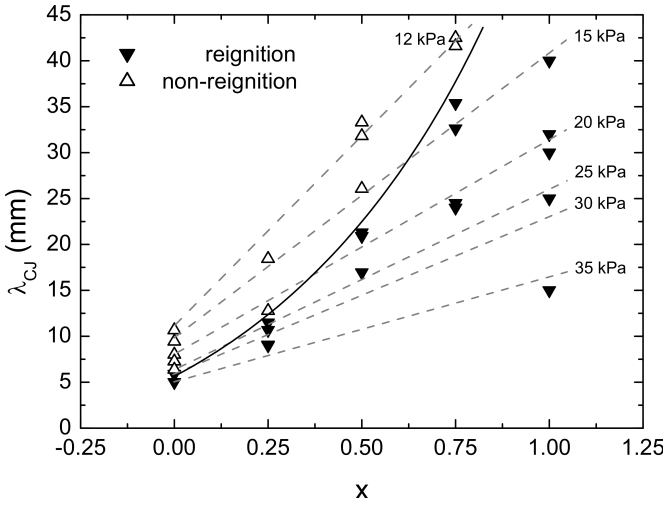

Fig. 5 Re-ignition domain for the mixtures (1-x)H_2 + xCH_4 + $\frac{1}{2}$ (1 + 3 x)O_2 in the plane Composition (x) - CJ cell mean width (λ_{CJ}) depending on the initial pressure (Plate A, $e = 7$ mm, $N = 64$, $d = 3$ mm, Table 1).

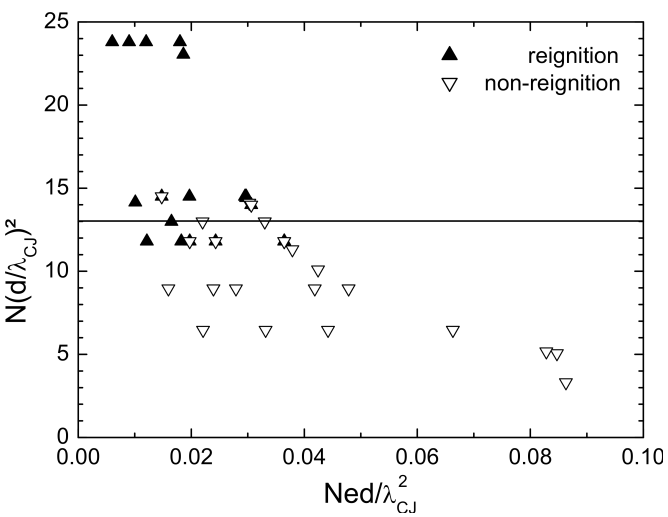

Fig. 6 Non-dimensional re-ignition domain for the mixture H_2 + $\frac{1}{2}$ O_2 ($x = 0$) in the plane Surface dissipation - re-ignition surface taking into account the properties of all plates (Table 1).

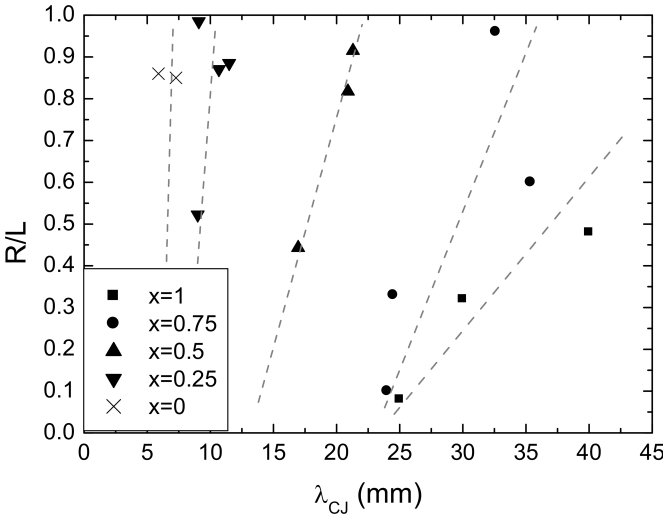

Fig. 7 Non-dimensional re-ignition distance R/L as a function of the mean detonation cell size λ_{CJ} for the mixtures (1-x)H_2 + xCH_4 + $\frac{1}{2}$ (1 + 3 x)O_2.

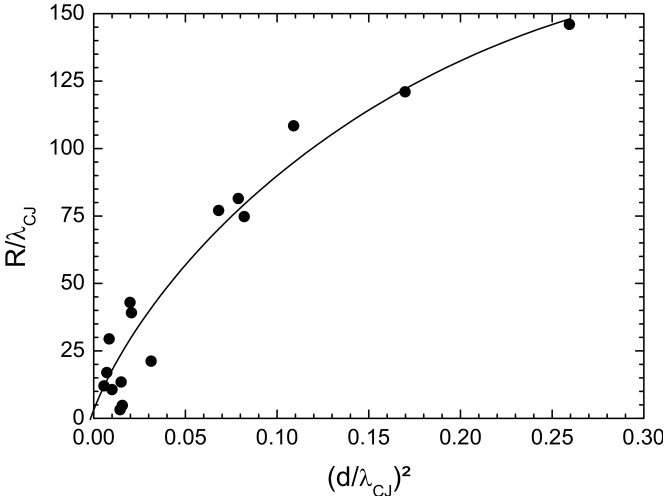

Fig. 8 Non-dimensional re-ignition distance as a function of the re-ignition-surface non-dimensional parameter for the mixtures (1-x)H_2 + xCH_4 + $\frac{1}{2}$ (1 + 3 x)O_2 with the values of x=0, 0.25, 0.5, 0.75 and 1 (Plate A, $e = 7$ mm, $N = 64$, $d = 3$ mm, Table 1).

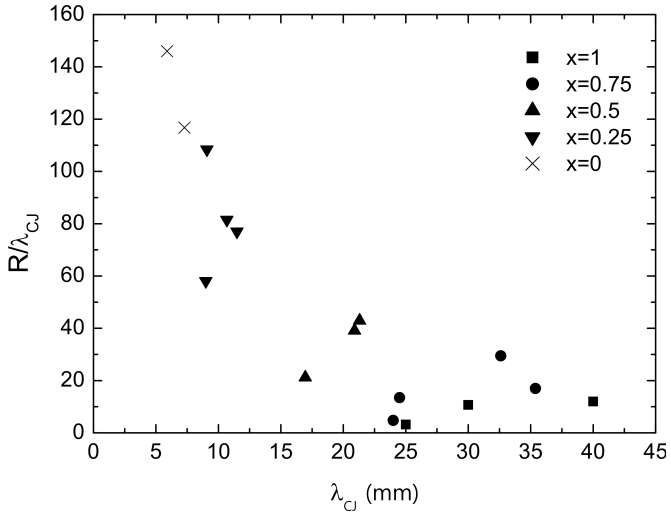

Fig. 9 Non-dimensional re-ignition distance for the mixtures (1-x)H_2 + xCH_4 + $\frac{1}{2}$ (1 + 3 x)O_2 as a function of the cell mean width λ_{CJ}. (Plate A, $e = 7$ mm, $N = 64$, $d = 3$ mm, Table 1).

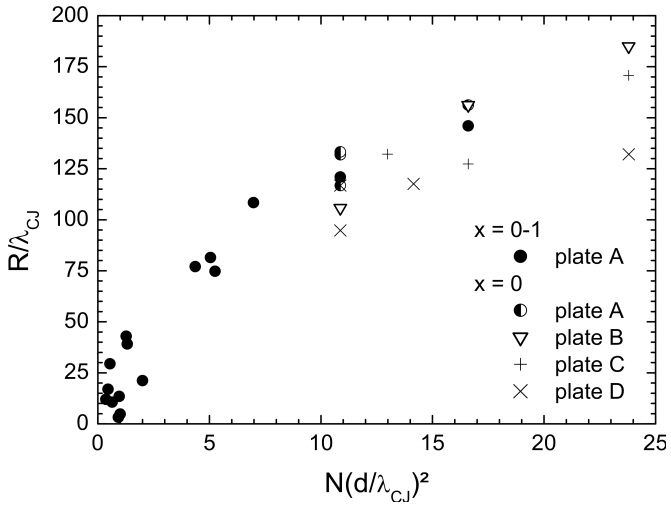

Fig. 10 Non-dimensional re-ignition distance as a function of the re-ignition-surface non-dimensional parameter for the mixtures (1-x)H_2 + xCH_4 + $\frac{1}{2}$ (1 + 3 x)O_2 for all plates (Table 1).